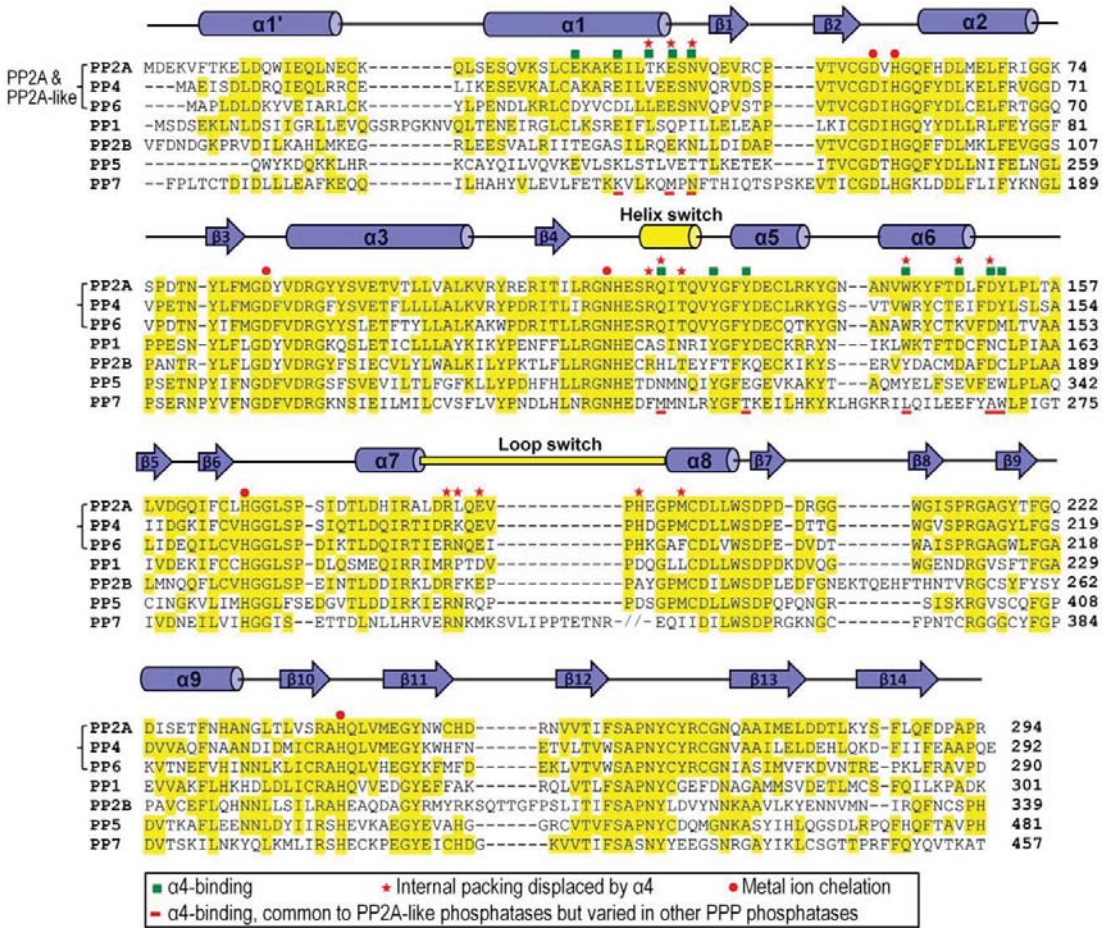

Supplementary Figure S1. Sequence alignment of the catalytic subunit of PP2A with other members of the PPP family Ser/Thr phosphatases of human origin. Secondary structural elements of the catalytic subunit of PP2A are indicated above the sequences. Conserved residues are highlighted inyellow. Residues that participate in α4-binding are indicated by green squares. Residues whose internal packing is displaced by α4 are indicated by red stars. α4-binding residues common to PP2A-like phosphatases but varied in other members of the PPP family phosphatases are underlined by red lines. Catalytic metal ion chelating residues are identified by red circles.

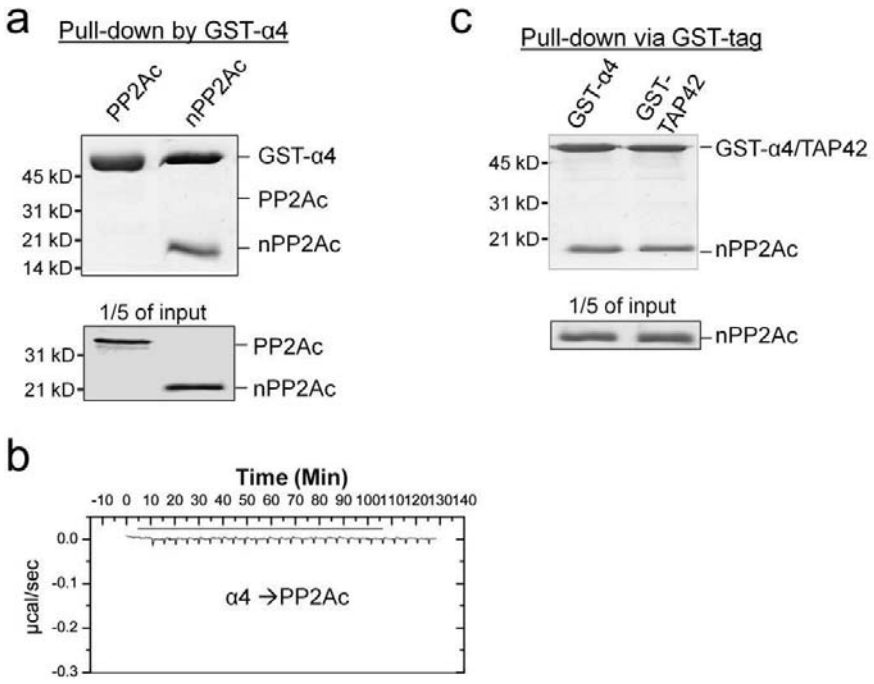

Supplementary Figure S2. Interaction of α4 with active, full-length PP2Ac and nPP2Ac (PP2Ac 1-153). (a) Pull-down of active and nPP2Ac by GST-tagged α4. The bound protein samples and protein inputs for pull-down were visualized on SDS-PAGE by Coomassie blue staining. (b) Isothermal titration calorimetry does not detect interaction between active PP2Ac and α4. (c) Pull-down of nPP2Ac by GST-tagged α4 and TAP42 similar to (a).

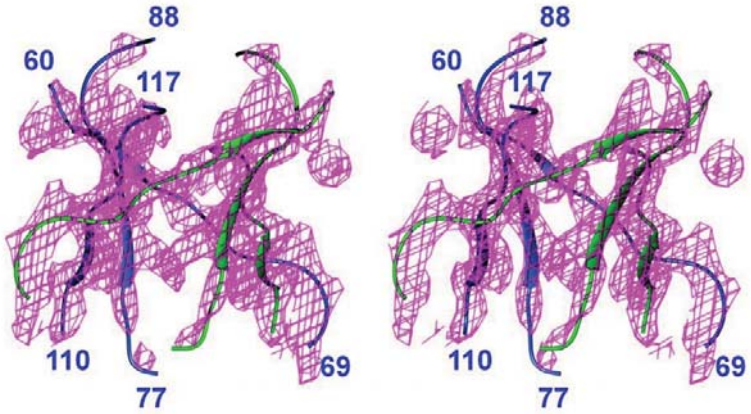

Supplementary Figure S3. The β-sheet in the nPP2Ac- α4 complex (blue) and the self-associated, symmetry-related β-sheet (green) in ribbon. The 2Fo-Fc electron density map at 2.0σ is shown and colored magenta.

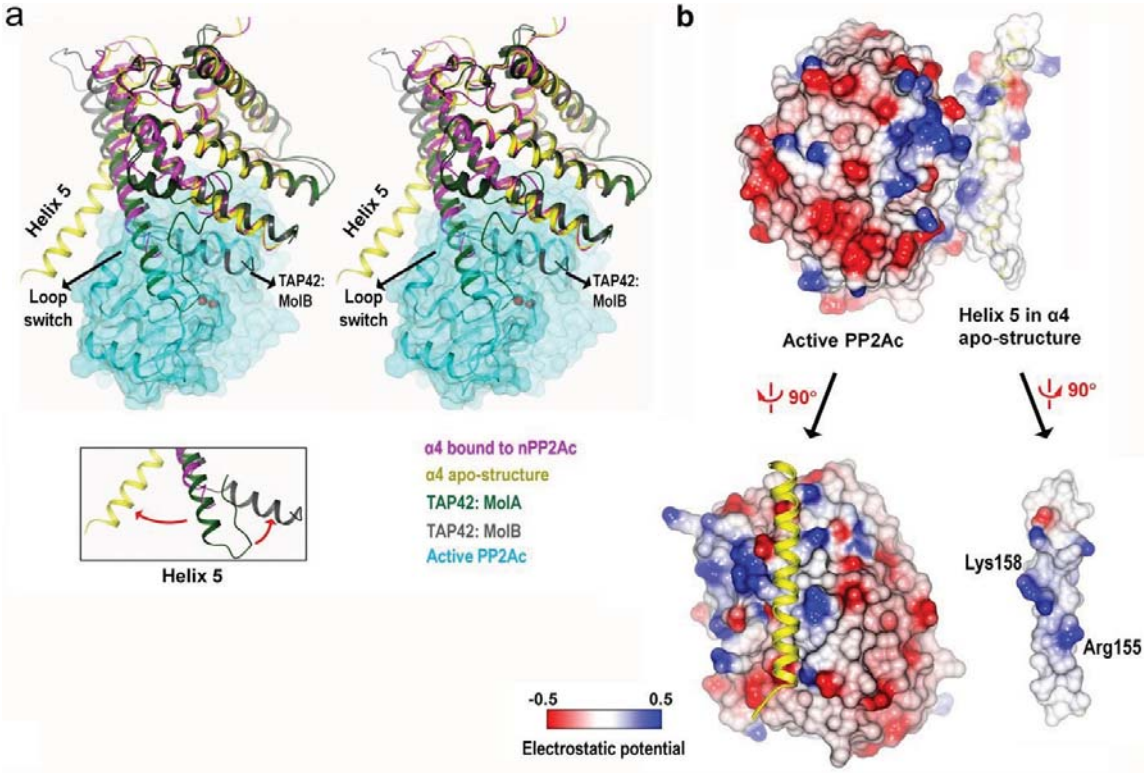

Supplementary Figure S4. None of various conformations of α4/TAP42 is compatible for binding with active PP2Ac. (**a**) Alignment of structures of the nPP2Ac-α4 complex, α4 apo-structure (3QC1) and two different conformations of TAP42 (2V0P: MolA and MolB) via α4 helix 1-4. The structure of active PP2Ac is aligned with the nPP2Ac-α4 complex via the unaltered helices in the helix motif of PP2Ac. All models are shown in ribbon and colored as indicated except that active PP2Ac is also shown in semi-transparent surface. Conformational variation in helix 5 of α4/TAP42 is highlighted (inlet, lower left). Helix 5 of TAP42/MolA overlaps with that of nPP2Ac-bound α4 while that of TAP42/MolB clashes into the helix motif of PP2Ac, suggesting that TAP42 interacts with PP2Ac using MolA conformation. (**b**) Electrostatic potential shows minor overlaps but repulsive electrostatic contacts between active PP2Ac and helix 5 of α4 apo-structure. Helix 5 of α4 apo-structure is shown in ribbon (lower left) to indicate its relative position to active PP2Ac.

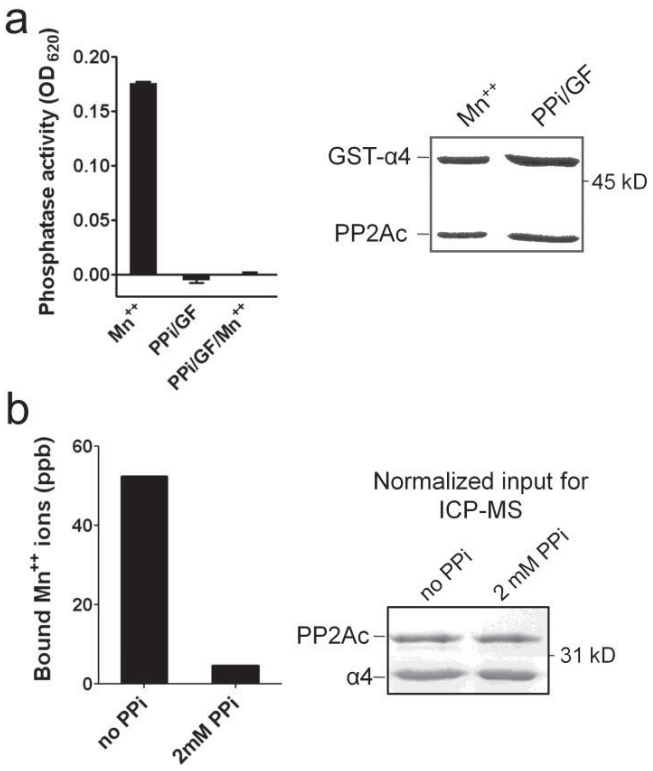

Supplementary Figure S5. α4-bound PP2Ac was stabilized in a metal-vacant, inactive form. (**a**) Phosphatase activity of the GST-α4/PP2Ac purified over gel filtration column after inactivation by PPi at 37°C for 10 minutes (PPi/GF) followed by re-activation by Mn^{++} (PPi/GF/Mn^{++}). The mixture of GST-α4 and PP2Ac incubated in the presence of 50 μM Mn^{++} at 37°C for 10 minutes (Mn^{++}) was used as control. The sample inputs for the phosphatase assay are visualized on SDS-PAGE by Coomassie blue staining. (**b**) ICP-MS determines the metal content of PP2Ac mixed with α4 prior to and after inactivation by 2 mM PPi at 37°C for 10 minutes followed by re-activation by Mn^{++}. Free metal ions were removed by gel filtration prior to ICP-MS analysis. The normalized inputs for α4 and PP2Ac for ICP-MS were visualized on SDS-PAGE by Coomassie blue staining.

Supplementary Table S1. Crystallographic data collection, phasing, and refinement.

Data Collection and Phasing	
Crystal	α4-PP2Ac (1-153)
Data set	SeMet SAD
Space group	P3221
Unit Cell	
a/b/c	116.127/116.127/81.230
α/β/γ	90.00/90.00/120.00
Wavelength (Å)	0.9792
Resolution (Å)	50.0-2.797 (2.85-2.797)
Unique observations	15948 (777)
Redundancy	20.1 (10.7)
R-symm[1]	0.070 (0.545)
Completeness (%)	99.8 (98.7)
I/SigI	28.7 (3.22)
Phasing	
Anomalous signal	1.63 (0.70)
Figure of merit	0.65
Refinement	
Resolution (Å)	37.7-2.797
No. reflections (free)	15885 (796)
Completeness (%)	99.54 (98.01)
R-factor (%)	17.87
R-free (%)	22.24
Number of atoms (total)	2708
Protein	2674
Water	34
RMSD bond lengths (Å)	0.009
RMSD bond angles (°)	1.21
Average B-factors (with TLS contribution) (Å^2)	84.5
Ramachandran plot:	
Preferred regions (%)	94.0
Allowed regions (%)	5.02
Outliers (%)	0.98

X-ray diffraction data were collected on one crystal. Values in parentheses are for highest-resolution shell.